

Discovery of 1-((6-Aminopyridin-3-yl)methyl)-3-(4-Bromophenyl) Urea as a Potent, Irreversible Myeloperoxidase Inhibitor[§]

Martin L. Marro,¹ Andrew W. Patterson,¹ Lac Lee, Lin Deng, Aimee Reynolds, Xianglin Ren, Laura Axford, Anup Patnaik, Micah Hollis-Symynkywicz, Nigel Casson, Dominique Custeau, Lisa Ames, Sally Loi, Lihe Zhang, Toshiyuki Honda, Jutta Blank, Tyler J. Harrison, Julien P. N. Papillon, Lawrence G. Hamann, Jovita Marcinkeviciene, and Jean B. Regard

Cardiovascular and Metabolic Diseases (M.L.M., L.L., X.R., L.Ax., M.H.-S., N.C., D.C., L.Am., S.L., L.Z., T.H., J.M., J.B.R.), Global Discovery Chemistry (A.W.P., A.P., T.J.H., J.P.N.P., L.G.H.), PK Sciences (L.D.), Technical R&D (A.R.), and Chemical Biology and Therapeutics (J.B.), Novartis Institutes for BioMedical Research, Cambridge, Massachusetts

Received February 16, 2018; accepted August 1, 2018

ABSTRACT

Myeloperoxidase (MPO) is a leukocyte-derived redox enzyme that has been linked to oxidative stress and damage in many inflammatory states, including cardiovascular disease. We have discovered aminopyridines that are potent mechanism-based inhibitors of MPO, with significant selectivity over the closely related thyroid peroxidase. 1-((6-Aminopyridin-3-yl)methyl)-3-(4-bromophenyl)urea (Aminopyridine 2) inhibited MPO in human

plasma and blocked MPO-dependent vasomotor dysfunction *ex vivo* in rat aortic rings. Aminopyridine 2 also showed high oral bioavailability and inhibited MPO activity *in vivo* in a mouse model of peritonitis. Aminopyridine 2 could effectively be administered as a food admixture, making it an important tool for assessing the relative importance of MPO in preclinical models of chronic inflammatory disease.

Introduction

Myeloperoxidase (MPO) is a heme-containing peroxidase that is present in phagocytic cells, where it participates in the innate immune response. In neutrophils, MPO is stored in azurophilic granules, and it has been reported to represent 5% of total cellular protein (Schultz and Kaminker, 1962). MPO is a homodimeric cationic glycoprotein that binds readily to bacterial and mammalian cell surfaces. The primary antimicrobial function of MPO is achieved by catalyzing the oxidation of halides such as chloride (Cl^-) or bromide (Br^-) ions by hydrogen peroxide (H_2O_2) to produce hypochlorous (HOCl) or hypobromous acids, respectively. Upon activation of phagocytes, MPO activity is detectable both in phagosomes and extracellularly, where it can remain or transcytose into interstitial compartments, and its enzymatic products can oxidize proteins, lipids, nucleic acids, and other small molecules.

Beyond clearance of pathogens, acute and chronic MPO activation is associated with generating oxidants within tissues, potentially contributing to the pathogenesis of inflammatory disease. Human DNA polymorphism associations and pharmacological data implicate aberrant MPO activity in inflammatory diseases such as cystic fibrosis, chronic obstructive

pulmonary disease, Parkinson's disease, rheumatoid arthritis, acute kidney injury, and atherosclerosis (Klebanoff, 2005). A role for MPO is particularly compelling in cardiovascular disease (Nussbaum et al., 2013). It has been suggested that MPO deficiency in humans is associated with a lower incidence of cardiovascular disease (Kutter et al., 2000; Rudolph et al., 2012), and MPO-deficient mice are protected in a model of myocardial infarction (Askari et al., 2003). Furthermore, elevated circulating MPO levels are associated with increased cardiovascular mortality in patients (Haslacher et al., 2012), and transgenic overexpression of MPO in hematopoietic cells exacerbates atherogenesis in mice (McMillen et al., 2005; Castellani et al., 2006).

The mechanisms by which MPO contributes to cardiovascular disease is not clear, but a number of hypotheses have been proposed. It has been suggested that MPO can oxidize high-density lipoprotein, thereby reducing its ability to efflux cholesterol (Shao et al., 2010). Moreover, HOCl can oxidize apolipoprotein B100, leading to increased uptake of oxidized low-density lipoproteins by macrophages, potentially leading to foam cell formation (Marsche et al., 2003), which is a hallmark of atherosclerosis. MPO has also been suggested to impair endothelial function by consuming nitric oxide (Eiserich et al., 2002) and/or promoting endothelial apoptosis (Sugiyama et al., 2004). Finally, there is evidence to suggest that MPO can activate matrix metalloproteinases

¹M.L.M. and A.W.P. contributed equally to this work.

<https://doi.org/10.1124/jpet.118.248435>.

§ This article has supplemental material available at jpet.aspetjournals.org.

ABBREVIATIONS: Aminopyridine 1, 1-((6-aminopyridin-3-yl)methyl)-3-(3-fluorophenyl)urea; Aminopyridine 2, 1-((6-aminopyridin-3-yl)methyl)-3-(4-bromophenyl)urea; DMSO, dimethylsulfoxide; Em, emission; EPO, eosinophil peroxidase; ESI, electrospray ionization; Ex, excitation; H_2O_2 , hydrogen peroxide; HOCl, hypochlorous; k_3/k_4 , partition ratio; k_{obs} , first-order rate constant of enzyme inactivation; LC, liquid chromatography; MPO, myeloperoxidase; MS, mass spectrometry; MS/MS, tandem mass spectrometry; m/z , mass/charge ratio; TPO, thyroid peroxidase.

and inactivate tissue inhibitors of metalloproteinases, resulting in reduced vessel wall extracellular matrix (Wang et al., 2007; Ehrenfeld et al., 2009). One or more of these mechanisms may play a role in atherosclerotic plaque instability and rupture, ultimately contributing to coronary artery disease, peripheral artery disease, heart failure, and stroke. Given the significant unmet medical need to treat inflammatory cardiovascular disease, we undertook the development of MPO inhibitors.

Mechanism-based irreversible inhibitors rely on the chemistry of the active site of the enzyme and are often highly selective for the target (Copeland, 2005). MPO mechanism-based irreversible inhibition involves initial oxidation of an inhibitor by the highly oxidizing compound I form of MPO to a short-lived radical (Fig. 1A). This intermediate radical can crosslink to the MPO protein or heme group, forming a covalent bond that irreversibly inhibits enzymatic activity.

To date, the most potent and specific MPO inhibitors that show robust in vivo activity are thiouracil-based, irreversible mechanism-based inhibitors (Tiden et al., 2011; Churg et al., 2012; Stefanova et al., 2012; Jucaite et al., 2015; Ruggeri et al., 2015; Zheng et al., 2015), the most advanced of which at the time of the writing of this manuscript are AZD3241 ([1-(2-isopropoxyethyl)-2-thioxo-1,2,3,5-tetrahydro-4H-pyrrolo [3,2-d]pyrimidin-4-one)] (Johnstrom et al., 2015; Jucaite et al., 2015; Kaindlstorfer et al., 2015) (<https://ncats.nih.gov/files/AZD3241-2016.pdf>) and PF-06282999 ([2-(6-(5-chloro-2-methoxyphenyl)-4-oxo-2-thioxo-3,4-dihydropyrimidin-1(2H-yl)acetamide)] (Ruggeri et al., 2015; Dong et al., 2016) (Fig. 1B). In this chemotype, the thioxo functionality undergoes

one-electron oxidation to generate a sulfur-based radical that crosslinks the heme group of MPO (Tiden et al., 2011; Geoghegan et al., 2012). Inhibitors from this class have advanced to clinical studies in patients with Parkinson's disease (Jucaite et al., 2015), multiple system atrophy (ClinicalTrials.gov, NCT02388295), and cardiovascular diseases (Dong et al., 2016).

Given the success of irreversible inhibitors to demonstrate in vivo efficacy, we sought to discover novel classes of irreversible MPO inhibitors with increased potency, selectivity against thyroid peroxidase (TPO), and suitable pharmacokinetic properties for in vivo testing. Here we describe the discovery of a novel chemical class of mechanism-based irreversible MPO inhibitor: the 2-aminopyridine class [i.e., 1-((6-aminopyridin-3-yl)methyl)-3-(3-fluorophenyl)urea (Aminopyridine 1)] (Fig. 1B). We further describe the preclinical characterization of 1-((6-aminopyridin-3-yl)methyl)-3-(4-bromophenyl)urea (Aminopyridine 2), a potent and selective MPO inhibitor with high oral exposure and in vivo activity.

Materials and Methods

Synthesis of 2-Aminopyridine Analogs

Aminopyridine 1.

To 3-fluoroaniline (0.020 g, 0.18 mmol) in dichloromethane (1.0 ml, 0.18 M) was added carbonyldiimidazole (0.037 g, 0.23 mmol), and the solution was stirred for 30 minutes at 0°C. Tert-butyl (5-(aminomethyl)pyridin-2-yl)carbamate (0.034 g, 0.15 mmol) and triethylamine (32 μ l, 0.23 mmol) were added, and the solution was stirred at room temperature for 16 hours. Trifluoroacetic acid (1.0 ml) was

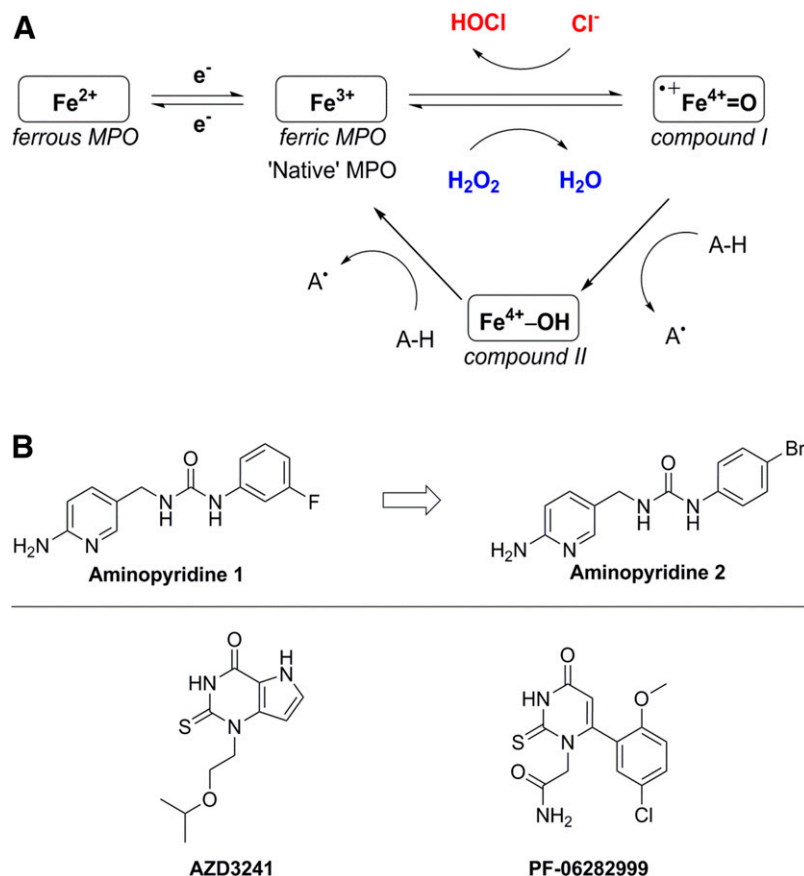


Fig. 1. The MPO catalytic cycle and chemical structures of interest. (A) "Native" MPO reacts with H_2O_2 to form compound I, a highly oxidative and reactive species. Compound I can return to its native state by reacting with a halogen, such as chloride, or via two electron reductions, with compound II as an intermediate. (B) The structures for Aminopyridines 1 and 2 and advanced thiouracils are shown.

added, and the solution was stirred overnight at room temperature. The reaction solution was concentrated under vacuum, and the residue was purified by preparative high-performance liquid chromatography (HPLC) using a gradient of acetonitrile/H₂O (0.1% NH₄OH) to give 0.011 g of Aminopyridine 1 (23%). Mass spectrometry (MS) [electrospray ionization (ESI), positive ion] *m/z*: 261.1 (M + 1); ¹H NMR [400 MHz, dimethylsulfoxide (DMSO)-d₆] δ ppm: 4.08 (d, J = 5.8 Hz, ²H); 5.84 (s, ²H); 6.40 (d, J = 8.3 Hz, ¹H); 6.52 (t, J = 5.7 Hz, ¹H); 6.64–6.73 (m, ¹H); 7.01 (ddd, J = 8.2, 1.9, 0.9 Hz, ¹H); 7.23 (td, J = 8.2, 7.0 Hz, ¹H); 7.32 (dd, J = 8.5, 2.5 Hz, ¹H); 7.45 (dt, J = 12.2, 2.3 Hz, ¹H); 7.84 (d, J = 2.0 Hz, ¹H); and 8.71 (s, ¹H). A purity of >99% was routinely achieved (Supplemental Fig. 1A).

Aminopyridine 2.

To tert-butyl (5-(aminomethyl)pyridin-2-yl)carbamate (0.190 g, 0.851 mmol) in dichloromethane (6 ml, 0.14 M) was added 1-bromo-4-isocyanatobenzene (0.169 g, 0.851 mmol), and a white precipitate formed immediately. The mixture was stirred at room temperature for 30 minutes and then concentrated. The resulting white solid was then suspended in acetonitrile (2 ml, 0.43 M), aqueous HBr (48%, 1 ml) was added, and the mixture was stirred at room temperature for 15 hours. The solution was then made basic with saturated aqueous ammonium hydroxide, and the resulting solid was collected by vacuum filtration washing with water and acetonitrile. Further drying under vacuum yielded 0.214 g of Aminopyridine 2 (77%) as a white solid. MS [(ESI), positive ion] *m/z*: 321.0 (M + H), 323.0 (M + H); ¹H NMR (400 MHz, DMSO-d₆) δ ppm: 4.08 (d, J = 5.7 Hz, ²H); 5.84 (s, ²H); 6.41 (dd, J = 8.6, 0.8 Hz, ¹H); 6.49 (t, J = 5.8 Hz, ¹H); 7.29–7.43 (m, ⁵H); 7.84 (d, J = 2.3 Hz, ¹H); 8.63 (s, ¹H); ESI high-resolution MS *m/z* calculated for C₁₃H₁₄N₄OBr [M + 1] 321.0351; found 321.0340. A purity of >99% was routinely achieved (Supplemental Fig. 1B).

MPO Peroxidation Assay. In a Costar black 384-well plate (catalog no. 3573; Corning, Corning, NY) we combined 10 mM phosphate buffer (pH 7.4) with human MPO (catalog no. CSI19692; Cell Sciences, Newburyport, MA), Amplex Red Reagent (catalog no. A12222; Thermo Fisher Scientific, Waltham, MA), and H₂O₂ to final concentrations of 2.5 nM, 10 μM, and 6.7 μM, respectively. MPO inhibitor compounds were added from a DMSO stock, and the reactions were read on a SpectraMax Fluorescence Plate Reader [wavelengths: excitation (Ex) 563 nm; emission (Em) 587 nm; Molecular Devices, Sunnyvale, CA]. Endpoint relative fluorescence units were measured at 180 seconds to calculate inhibition curves, and the remaining MPO activity was calculated as %Activity = [(read – minimum)/(maximum – minimum)] × 100.

TPO Peroxidation Assay. In a Costar black 384-well plate (catalog no. 3573; Corning), we combined 10 mM phosphate buffer (pH 7.4) with human TPO (catalog no. CSI11064; Cell Sciences), Amplex Red Reagent (catalog no. A12222; Thermo Fisher Scientific), and H₂O₂ to final concentrations of 25 nM, 20 μM and 6.7 μM, respectively. MPO inhibitor compounds were added from a DMSO stock, and the reactions were read on a SpectraMax Fluorescence Plate Reader (Ex 563 nm; Em 587 nm; Molecular Devices). Endpoint relative fluorescence units were measured at 180 seconds to calculate inhibition curves, and the remaining TPO activity was calculated as %Activity = [(read – minimum)/(maximum – minimum)] × 100.

Reversibility by Dialysis. Human MPO (catalog no. 426-10; Lee Biosolutions, Maryland Heights, MO), MPO inhibitor (from a DMSO stock), and H₂O₂ were combined with 100 mM phosphate buffer (pH 7.4) to final concentrations of 1, 20, and 30 μM, respectively. After a 10-minute reaction time, 100 μM ascorbic acid was added to quench the reaction, which was then cassette dialyzed (catalog no. 66383; Thermo Scientific) for 72 hours in 0.5 l of 100 mM phosphate buffer (pH 7.4). Residual MPO activity could be determined by performing a 1:200 dilution of the dialyzed sample (final concentration 5 nM MPO) into 10 mM phosphate buffer (pH 7.4) containing 10 μM Amplex Red Reagent and 6.7 μM H₂O₂. Reactions were then read using a SpectraMax M5e Plate Reader (Ex 563 nm; Em 590 nm; Molecular Devices), and all experiments were performed in duplicate.

Stopped Flow. Experiments were performed on a Stopped Flow Instrument (Kintek, Snow Shoe, PA) with three syringes, each

allowing equal volume mixing of 40 nM MPO, 40 μM H₂O₂/40 μM Amplex Red Reagent, and variable concentration of aminopyridine in DMSO. Fluorescence was monitored for 5 seconds after mixing (Ex 563 nm; Em 587 nm) recording four to five replicates at each compound concentration. The early, linear fluorescence values were fit to this equation: [P] = V_i/k_{obs}[1 – exp(–k_{obs}t)], where P is the product, V_i is the initial reaction velocity (in RFU/s), t is time (in seconds), and k_{obs} is the first-order rate constant of enzyme inactivation. k_{obs} data were then fit to the equation k_{obs} = (k_{inact} × [I])/(K_i + [I]), where [I] is the inhibitor concentration to determine k_{inact}/K_i.

Partition Ratio. To eliminate chloride salt, human MPO (catalog no. 426-10; Lee Biosolutions) was dialyzed with a 500-fold excess volume of 100 mM phosphate buffer (pH 7.4) for 8 hours, and this was repeated two additional times. One hundred nanomolar MPO, 0.53 mM H₂O₂, and aminopyridine were incubated in 100 mM phosphate buffer (pH 7.4) at room temperature for 10 minutes. One microliter of this MPO/H₂O₂/compound solution was then added to a Costar 384-well plate (catalog no. 3573; Corning) along with 99 μl of a solution containing 10.1 μM Amplex Red Reagent and 10.1 μM H₂O₂ in 10 mM phosphate buffer (pH 7.4). The plate was read on a SpectraMax Fluorescence Plate Reader (Ex 563 nm; Em 587 nm; Molecular Devices) recording five 75-second reads each (total 300 seconds); only the initial rate was used for analysis. The remaining MPO activity was calculated as %Activity = [(read – minimum)/(maximum – minimum)] × 100, and %Activity was plotted as a function of the ratio [inhibitor]/[MPO] in XLfit (Excel; Microsoft, Redmond, WA). The point at which the percentage of activity becomes 0 indicates the number of moles of inhibitor required to inactivate 1 mol of enzyme (1 + r). This value was used to determine the partition ratio r.

MPO Plasma Assay. This assay is conceptually similar to one previously published (Franck et al., 2009). Briefly, Reacti-Bind Pierce black 96-well G protein-coated plates (catalog no. 15157; Thermo Fisher Scientific) were washed with 150 mM NaCl + 0.1% Tween-20 (wash buffer pH 7.4) and incubated at room temperature with either anti-mouse MPO antibody (5 μg/ml; catalog no. AF3667; R&D Systems, Minneapolis, MN) or anti-human MPO antibody (5 μg/ml; catalog no. AF3174; R&D Systems) in 100 μl of Pierce SuperBlock buffer with 0.05% Tween-20 (catalog no. 37535; Thermo Fisher Scientific) for 2 hours. Wells were washed four times with PBS buffer (pH 7.4). For MPO IC₅₀ studies, 1 nM MPO, 1 mM H₂O₂, and compound in increasing concentrations were mixed with heparinized human plasma (isolated from healthy volunteers, pooled from n = 10 donors), and 100 μl was added per well. The plate was then incubated at 37°C for 2 hours. The plates were washed again four times with wash buffer, 100 μl of detection reagent [50 mM phosphate buffer (pH 7.4), 40 μM Amplex UltraRed Reagent (catalog no. A36006; Thermo Fisher Scientific), 10 μM H₂O₂, and 10 mM sodium nitrite] was added to each well, and the plate was read on a SpectraMax M5e Plate Reader (Ex 563 nm; Em 590 nm; Molecular Devices). Under these conditions, data were linear for at least 40 minutes.

Heme Modification. To eliminate chloride salt human MPO (catalog no. 426-10; Lee Biosolutions) was dialyzed with three exchanges of 500-fold excess volume of 100 mM phosphate buffer (pH 7.4) for a total of 24 hours. UV-visible absorption spectra (Cary 50; Agilent Technologies, Santa Clara, CA) of MPO (1 μM) was recorded as a baseline and then 20 μM Aminopyridine 2 was added, followed by 30 μM H₂O₂ and 1 mM ascorbic acid. The absorption spectrum was then measured again after a 10-minute incubation in a cell with a 1-cm path length.

Pharmacokinetic Studies. All experiments involving animals were conducted in our Association for Assessment and Accreditation of Laboratory Animal Care-accredited facilities, in accordance with the *Guide for the Care and Use of Laboratory Animals* as adopted and promulgated by the U.S. National Institutes of Health and were approved by the Novartis Animal Care and Use Committee. C57BL/6 mice or Sprague-Dawley rats (Harlan Laboratories, Indianapolis, IN) were administered compound either intravenously (1 mg/kg; a solution in 30% polyethylene glycol 300, 10% Cremophor EL in PBS) or by oral gavage (10 mg/kg; a suspension in 0.1% Tween-80, 0.5%

methylcellulose in water). Similarly, purpose-bred beagle dogs were administered compound either intravenously [0.3 mg/kg; 10% 0.1 N HCl, 20% polyethylene glycol 300, 10% Solutol (Sigma-Aldrich, St. Louis, MO), in PBS] or by oral gavage (10 mg/kg; 0.5% Tween-80/0.5% methyl cellulose, in water). Blood was collected in EDTA-coated capillary tubes. Plasma was isolated by centrifugation and frozen until analysis. Samples were prepared by liquid-liquid extraction and analyzed by LC-tandem MS (MS/MS) and concentrations of Aminopyridine 2 were determined by interpolation from a standard curve.

Aortic Ring Relaxation. Male Sprague-Dawley rats (Charles River, Wilmington, MA) were purchased at 8 weeks of age, housed two per cage under normal light cycle conditions (12 hours on, 12 hours off) and used within 6 weeks of arrival. Rats were anesthetized by isoflurane inhalation and euthanized by exsanguination, and the thoracic aorta was then isolated and transferred into modified Krebs-Henseleit buffer (KHB; 1.2 mM KH_2PO_4 , 27.2 mM NaHCO_3 , 119 mM NaCl, 4.6 mM KCl, 1.75 mM CaCl_2 , 1.2 mM MgSO_4 , 11.1 mM glucose, 0.03 mM Na_2EDTA). The aortae were then cleaned of fat and connective tissue, cut into 2- to 3-mm rings, and washed five times in KHB. Rings were then placed into KHB with 500 nM human MPO, 94 mM H_2O_2 , and Aminopyridine 2, and incubated at 37°C for 45 minutes. The rings were then washed an additional five times with KHB, and mounted onto an organ bath/isometric transducer chamber (Radnoti, Monrovia, CA). After equilibration, the rings were precontracted with 1 μM phenylephrine, and their ability to relax with increasing amounts of acetylcholine was assessed. As a final step, 30 nM sodium nitroprusside was added to each bath to confirm normal smooth muscle cell function.

Mouse Peritonitis. Male C57BL/6j or MPO null mice (Brennan et al., 2001) (both from Jackson Laboratories, Bar Harbor, ME) were purchased at 8 weeks of age, housed four per cage under normal light cycle conditions (12 hours on, 12 hours off) and used within 6 weeks of arrival. At time zero, peritonitis was induced by injection i.p. with 1 ml of thioglycolate broth (4% in water; catalog no. T9032; Sigma-Aldrich). After 19 hours, the mice were administered an Aminopyridine 2 suspension in vehicle or vehicle composed of 0.5% methyl cellulose, 0.1% Tween-80, in water by oral gavage. One hour later, the mice were injected with 0.5 ml zymosan A (10 mg/ml, i.p., in water; catalog no. Z4250; Sigma-Aldrich), and were euthanized with carbon dioxide after an additional 4 hours. Blood was drawn by cardiac puncture into heparinized tubes, and the plasma was isolated. The peritoneal cavity was flushed by lavage with 1.5 ml of ice-cold PBS containing 1 mM methionine and 0.01 mg/ml catalase. For long-term studies, Aminopyridine 2 was formulated into a western diet (D12079B; Research Diets Inc., New Brunswick, NJ) at 0.0417% (~50 mg/kg per day) or 0.1668% (~200 mg/kg per day) and fed to the mice for 2 weeks prior to the induction of peritonitis as described above.

3-Chlorotyrosine and Tyrosine Quantification. Peritoneal exudate (200 μl) was placed on an Amicon 3000 mol. wt. cutoff filter and centrifuged at 14,000g for 60 minutes at 4°C. Forty microliters of the filtrate was added to a new 1.5-ml Eppendorf tube followed by 5 μl of a 500 nM solution of $^{13}\text{C}_6$ -tyrosine and $^{13}\text{C}_6$ -chlorotyrosine (Cambridge Isotope Laboratories Inc., Tewksbury, MA) internal standard and 35 μl of borate buffer (200 mM borate in water, approximately pH 8.4) and then mixed by vortexing at moderate speed for 10 seconds. A final reaction of a 100- μl volume was achieved by adding 20 μl of derivatization reagent (6-aminoquinolyl-*N*-hydroxysuccinimidyl carbamate from an AccQ-Tag Ultra Derivatization Kit; Waters, Milford, MA). The tube was vortexed at moderate speed for 10 seconds and then incubated at 55°C in a heating block for 10 minutes. Chlorotyrosine and tyrosine were quantified on a LC-coupled (Shimadzu, Kyoto, Japan) QTRAP 6500 LC-MS/MS System (AB Sciex, Framingham, MA) using the peak area ratio relative to the internal standards and multiplied by 62.5 as an isotopic abundance factor. Additional technical details are provided in the Supplemental Material.

Statistical Analysis. Statistical test results are indicated in the text and figure legends (* $P < 0.05$, ** $P < 0.01$, *** $P < 0.001$).

Results

More than 1.4 million compounds were screened in a fluorescent MPO peroxidation biochemical assay with the goal of identifying MPO inhibitors. This screen and follow-up efforts yielded 4669 hits that were selected for mechanism of action and selectivity profiling. IC_{50} measurements were conducted with both MPO and TPO, which is a close homolog of MPO. Dilution experiments were designed to identify compounds that would inhibit MPO at a 20 μM compound concentration and retain inhibition after 1000-fold dilution (a behavior typical of irreversible inhibitors), and 133 compounds were identified that retained >50% inhibition of MPO activity.

One novel class of mechanism-based irreversible inhibitors that met the criteria of having an MPO $\text{IC}_{50} < 0.5 \mu\text{M}$, >100-fold selectivity against TPO, and irreversible inhibition confirmed by dialysis shared a 5-substituted-2-aminopyridine pharmacophore (i.e., Aminopyridine 1) (Fig. 1B). Aminopyridine 1 had a promising profile, with the rate of MPO inactivation (k_{inact}/K_i : 14,000 $\text{M}^{-1}\text{s}^{-1}$) matching that of clinical compound PF-06282999 [2-(6-(5-chloro-2-methoxyphenyl)-4-oxo-2-thioxo-3,4-dihydropyrimidin-1(2H)-yl)acetamide] (k_{inact}/K_i : 11,749 $\text{M}^{-1}\text{s}^{-1}$) (Ruggeri et al., 2015) (Fig. 1B) and the apparent MPO IC_{50} (0.45 μM) matching that of clinical compound AZD3241 (0.63 μM) (<https://ncats.nih.gov/files/AZD3241-2016.pdf>) (Fig. 1B) and having >200-fold selectivity over TPO (Table 1). The partition ratio (k_3/k_4) of Aminopyridine 1, which measures the efficiency of irreversible inhibition, was moderate (57). Thus, reducing the k_3/k_4 ratio and increasing k_{inact}/K_i ratio while maintaining selectivity over TPO, along with obtaining in vivo exposure, became the primary foci of our medicinal chemistry efforts. Optimization efforts resulted in Aminopyridine 2, which has a 4-bromo-substituted phenyl ring in place of the 3-fluoro substitution on Aminopyridine 1 (Fig. 1B). This small change provided a marked improvement in MPO k_{inact}/K_i (76,500 $\text{M}^{-1}\text{s}^{-1}$) and k_3/k_4 (11) kinetic values, while further increasing to >588-fold selectivity over TPO (Table 1). Aminopyridine 2 inhibited MPO peroxidase activity in vitro and in human plasma MPO activity ex vivo with apparent IC_{50} values of 0.16 and 1.9 μM , respectively (Fig. 2A).

Analysis of the activity of Aminopyridine 2 against additional oxidase targets found activity against eosinophil peroxidase (EPO; apparent $\text{IC}_{50} = 0.29 \mu\text{M}$) (Supplemental Fig. 2), but no apparent activity against cyclooxygenase 1, cyclooxygenase 2, CYP3A4, CYP2D6, CYP2C9, monoamine oxidase A, arachidonate 12-lipoxygenase, or arachidonate 5-lipoxygenase (data not shown).

The mechanism of inhibition was investigated by incubating Aminopyridine 2 (or DMSO alone) with MPO and H_2O_2 followed by dialysis and further dilution prior to analysis for MPO activity. Aminopyridine 2-dependent inhibition persisted after dialysis and dilution, suggesting an irreversible mechanism (Fig. 2B). The mechanism of MPO inhibition was further evaluated by plotting k_{obs} values relative to the concentration of Aminopyridine 2, allowing a determination of the k_{inact} rate of 2.2/s and K_i of 24 μM . Saturation was observed, indicating a two-step mechanism of inactivation (Fig. 2C). Furthermore, Aminopyridine 2 can form conjugates with 5,5-dimethyl-1-pyrroline N-oxide in the presence of MPO and H_2O_2 , which is consistent with the mechanism of inhibition involving an active radical intermediate (Supplemental Table 1).

To better understand the role of the heme moiety during inhibition, we explored the distinct spectral properties of the redox intermediates of MPO. When Aminopyridine 2 was added

TABLE 1

In vitro pharmacology data for Aminopyridine 1 and 2

Values were determined as described in the *Materials and Methods* section and presented as the geometric mean of at least three independent experiments.

Aminopyridine Compound	MPO IC ₅₀	MPO k_{inact}/K_i	MPO k_3/k_4	MPO Dialysis	TPO IC ₅₀	TPO Selectivity
	μM	$\text{M}^{-1}\text{s}^{-1}$		% recovered activity	μM	Fold
1	0.45	14,000	57	42	>100	>222
2	0.16	76,500	11	8	>100	>588

directly to MPO, no change in the UV-visible absorption spectrum was observed. Upon addition of H₂O₂, however, the Soret band shifted from 430 to 457 nm. Additionally, the second heme-specific peak at 570 nm shifted to 624 nm (Fig. 2D). The addition of ascorbic acid, which would normally reduce the higher heme oxidation states back to the native Fe(III) state, did not cause a shift back to 430 and 570 nm, indicating that the electronic properties of the heme group had been irreversibly altered by Aminopyridine 2 in the presence of H₂O₂ (Fig. 2D). Similar spectral shifts were seen for Aminopyridine 2 with EPO, but not with TPO (Supplemental Fig. 2), which is consistent with the enzymatic analysis. The nature of reactive species generated and subsequent alteration of the MPO heme environment is unclear and will require further experimentation, though initial analysis does not suggest an obvious modification to the heme group (data not shown).

Increased MPO activity has been linked to endothelial dysfunction and impaired vasomotor function in humans and preclinical models (Eiserich et al., 2002; Rudolph et al., 2012). Based on previous literature (Zhang et al., 2001), we developed an ex vivo model of MPO-dependent vasomotor dysfunction. Rat aorta was dissected and cut into rings that were then incubated in a modified KHB under various conditions. Incubation with either MPO or H₂O₂ alone did not impair acetylcholine-dependent relaxation, but incubation

with the combination of both MPO and H₂O₂ resulted in impaired relaxation (Fig. 3). MPO and H₂O₂ exposure did not impair smooth muscle cell relaxation in response to the direct nitric oxide donor sodium nitroprusside (data not shown), which is consistent with a direct effect of MPO and H₂O₂ on endothelial function. Aminopyridine 2 dose-dependently inhibited the MPO-dependent endothelial dysfunction while preserving vasomotor function (Fig. 3).

We evaluated the pharmacokinetics of Aminopyridine 2 in the mouse, rat, and dog. Low clearance, good oral exposure, and high oral bioavailability were observed across all three species (Supplemental Fig. 3; Table 2). The pharmacokinetic/pharmacodynamic relationship of Aminopyridine 2 was then evaluated in vivo in an induced peritonitis mouse model of acute inflammation. Mice were administered successive intraperitoneal doses of thioglycolate and zymosan A to promote neutrophil infiltration into the peritoneal cavity and degradation, respectively. Oral administration of 2.5, 25, 50, or 100 mg/kg Aminopyridine 2 1 hour prior to zymosan injection resulted in dose-dependent decreases in 3-chlorotyrosine accumulation in the peritoneal exudate (Fig. 4A), along with 24%, 62%, 74%, and 86% decreases in residual plasma MPO activity observed after 5 hours (Fig. 4B). The specificity of these endpoints was confirmed by the lack of detectable MPO activity in the exudate and plasma after the induction of

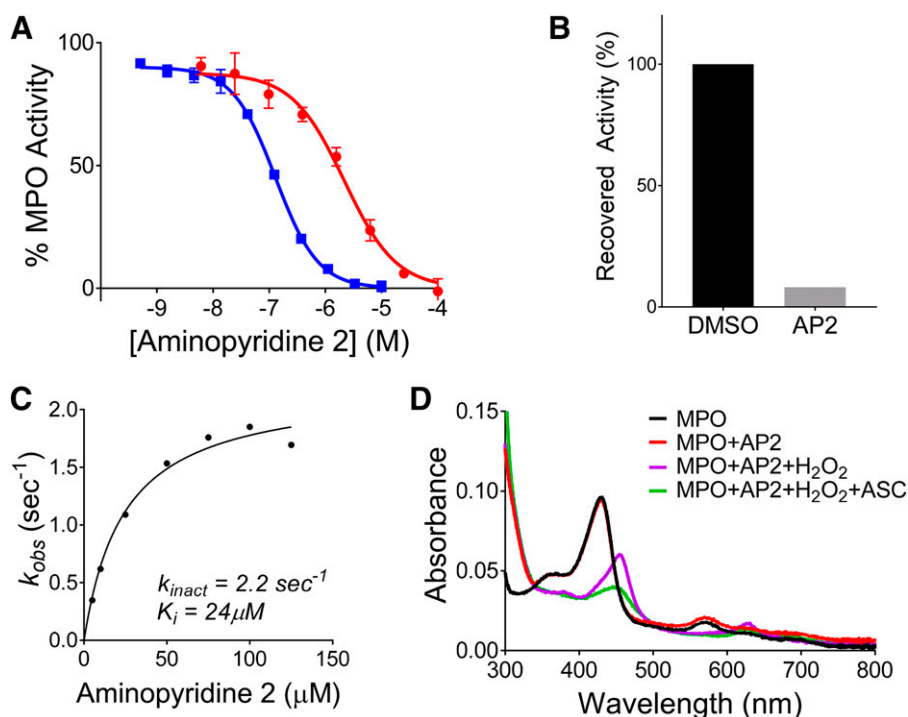


Fig. 2. Aminopyridine 2 (AP 2) irreversibly inhibits MPO. (A) Aminopyridine 2 was incubated with human MPO in phosphate buffer (peroxidation) or human plasma as described in *Materials and Methods*. MPO activity in the presence of H₂O₂ and Amplex Red Reagent was measured by fluorescence. Aminopyridine 2 inhibited MPO activity with an apparent IC₅₀ of 0.16 μM (blue squares), which shifted to 1.9 μM in the presence of human plasma (red circles). (B) Aminopyridine 2 (or DMSO vehicle) was incubated with human MPO and H₂O₂, followed by dialysis and dilution. Aminopyridine 2-dependent inhibition could not be reversed, suggesting irreversible inhibition. (C) k_{obs} values plotted as a function of Aminopyridine 2 concentration allowed the determination of k_{inact} and K_i values. (D) The incubation of MPO, H₂O₂, and Aminopyridine 2 results in a shift of the Soret peak and the formation of a new peak at 624 nm, which is consistent with a modification of MPO at or near the heme prosthetic group. ASC, ascorbic acid.

Discussion

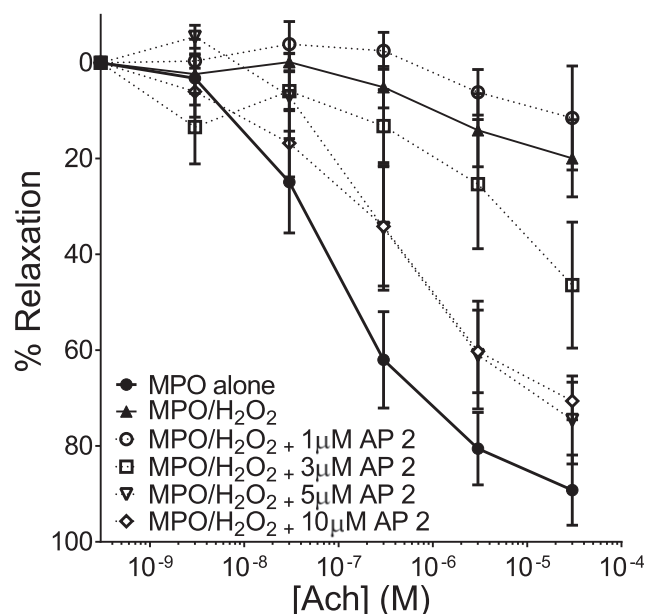


Fig. 3. Aminopyridine 2 (AP 2) prevents MPO-dependent endothelial dysfunction ex vivo. Rat aortic rings were preincubated with MPO, with or without H_2O_2 , and with or without Aminopyridine 2. The ability of the rings to constrict in response to phenylephrine and then relax in response to acetylcholine (Ach) was determined ex vivo in organ baths. Incubation of the rings with either MPO alone or H_2O_2 alone had no effect, whereas the combination resulted in an inability to respond to acetylcholine. The addition of Aminopyridine 2 dose-dependently blocked the MPO-dependent vasomotor dysfunction.

peritonitis in MPO-null mice (Fig. 4, A and B). Analysis of terminal plasma Aminopyridine 2 concentrations allowed us to calculate an apparent in vivo IC_{50} of $1.4 \mu M$ in the peritonitis model (Fig. 4C), which is similar to the human plasma IC_{50} (Fig. 2A).

To support long-term studies, we evaluated the potential to deliver Aminopyridine 2 in a food admixture. Aminopyridine 2 was formulated into a western diet (catalog no. D12079B; Research Diets), and mice were fed the control diet, the diet + 0.0417% (w/w) Aminopyridine 2 (~ 50 mg/kg per day), or the diet + 0.1668% (w/w) Aminopyridine 2 (~ 200 mg/kg per day) for 2 weeks. On day 14, peritonitis was induced in the mice, and MPO activity was assessed in both the peritoneal exudate and plasma. Aminopyridine 2 was able to dose-dependently inhibit both the accumulation of 3-chlorotyrosine in the peritoneal exudate (Fig. 4D) and plasma MPO activity (Fig. 4E), demonstrating that sufficient compound exposure to enable MPO inhibition and long-term efficacy studies could be achieved.

We screened a library of compounds with the goal of identifying novel mechanism-based irreversible inhibitors and identified 2-aminopyridines as one such class. Our data suggest that these aminopyridines fully and irreversibly inactivate MPO by modifying its heme environment. We demonstrate >500 -fold selectivity against TPO with Aminopyridine 2, suggesting an improved selectivity profile for this compound relative to known thiouracil-based inhibitors. Activity against EPO, however, suggests further selectivity profiling is warranted. Additionally, understanding the relevancy of Aminopyridine 2 potentially escaping the active site as a radical species and the likelihood of this posing a safety risk warrants further experimentation. Importantly, the aminopyridines described here potently and dose-dependently inactivated MPO in vivo, as demonstrated by the inhibition of MPO enzymatic activity in plasma and the formation of the HOCl-derived biomarker 3-chlorotyrosine in the peritoneum. Aminopyridine 2 also has excellent pharmacokinetic characteristics in rat, mouse, and dog, making it a promising tool for evaluating the role of MPO in models of inflammatory disease.

Neutrophil adhesion and degranulation is thought to promote functional changes in the vasculature, resulting in impaired vasomotor function and endothelial dysfunction. Upon secretion, MPO is found predominantly in the bloodstream, where it binds to high-density lipoprotein and the extracellular matrix of blood vessels. Previous data have suggested that vascular MPO can induce endothelial dysfunction and impaired vaso-relaxation (Eiserich et al., 2002). Although the precise mechanism is not clear, the consumption of endothelial cell-derived nitric oxide and direct oxidative damage to endothelial cells has been implicated. Here we developed an ex vivo model of MPO-dependent vasomotor dysfunction, demonstrating that both MPO and H_2O_2 are required to cause endothelial dysfunction and impair relaxation. Aminopyridine 2 was able to dose-dependently preserve vasomotor function and maintain a normal relaxation response to acetylcholine.

Given its high oral bioavailability, Aminopyridine 2 could be administered by daily oral gavage to support short studies or in food admixtures to support long-term studies. Aminopyridine 2 was effective in vivo in an acute model of inflammation (peritonitis). Using two assays of MPO inhibition (peritoneal Cl-Tyr and plasma MPO activity), we demonstrated clear dose-dependent enzymatic inhibition with Aminopyridine 2 by either oral gavage or food admixture. Collectively, these

TABLE 2

Summary of pharmacokinetic data for Aminopyridine 2 in preclinical species

The pharmacokinetics of Aminopyridine 2 in mice, rats, and dogs are summarized. Aminopyridine 2 concentrations were measured from plasma collected at specific time points, and pharmacokinetic parameters were calculated. All data are reported as the mean ($n = 2-3$).

Species	Oral C_{max} at 10 mg/kg	Oral T_{max} at 10 mg/kg	Oral AUC $0-\infty$	CLp	Vdss	$t_{1/2}$	Oral F
	nM	h	nM/h per milliliter	ml/min per kilogram	l/kg	h	%
Mouse	11,884	1.3	58,440	4.5	0.7	1.9	51
Rat	20,844	0.4	133,162	4.5	1.3	4.1	~ 100
Dog	19,486	2.3	335,615	1.9	0.9	7	~ 100

AUC, area under the curve; CLp, plasma clearance; Oral F, oral bioavailability; $t_{1/2}$, half-life; T_{max} , time to maximal concentration; Vdss, volume of distribution.

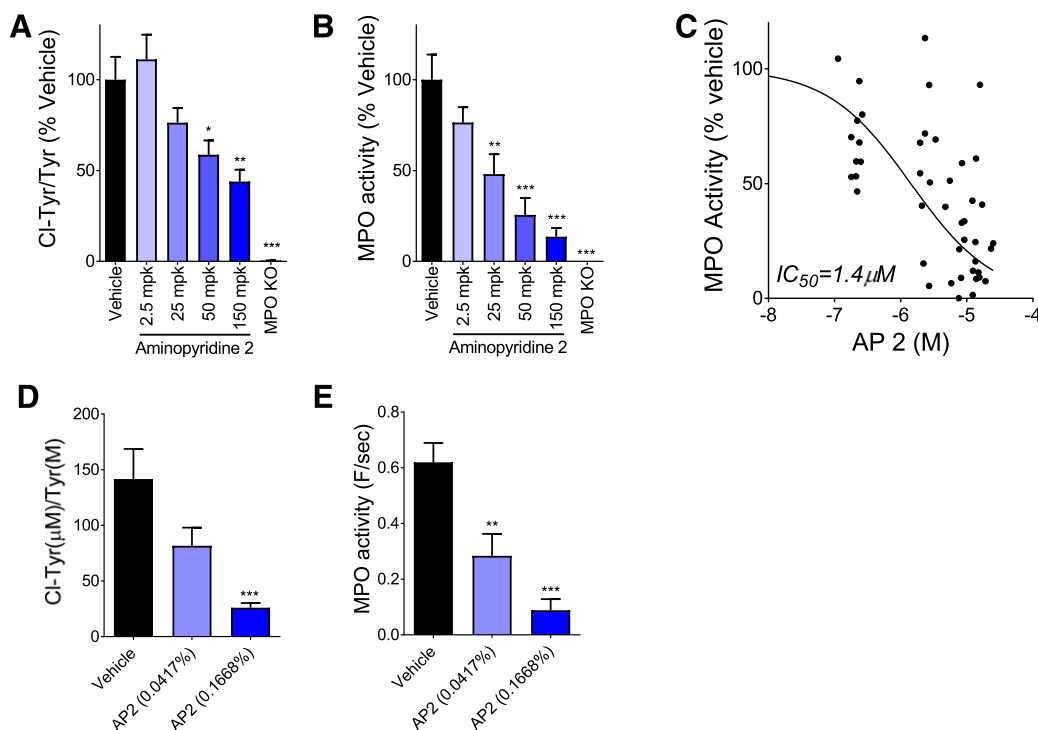


Fig. 4. Acute and chronic administration of Aminopyridine 2 (AP2) inhibits MPO activity in a mouse model of peritonitis. Aminopyridine 2 was dosed to mice orally ($n = 8-12$) just prior to zymosan A administration and MPO activity in the peritoneal exudate, and plasma was measured. Aminopyridine 2 dose-dependently inhibited 3-chlorotyrosine accumulation in the peritoneal exudate (A) and also inhibited residual MPO activity in the plasma 5 hours postdose (B). (C) There was an inverse relationship between total plasma Aminopyridine 2 concentration and plasma MPO activity, with the apparent in vivo IC_{50} estimated to be $1.4 \mu\text{M}$. Aminopyridine 2 was formulated as a food admixture and mice were fed ad libitum for 14 days. Aminopyridine 2 dose-dependently inhibited MPO activity in both peritoneal exudate by Cl-Tyr/Tyr ratio (D) and plasma by residual MPO activity (E). Data are presented as the mean \pm S.E.M., and statistical analyses were performed using one-way ANOVA. * $P < 0.05$ represents significance when compared with vehicle.

data suggest that aminopyridines can be effective inhibitors of MPO in vivo and good tools for elucidating the function of MPO in disease models.

Leukocyte-derived oxidants, including those produced by MPO, are associated with inflammatory disease in multiple tissue beds. We focused on MPO because there are significant clinical and preclinical data suggesting a potential role in the pathogenesis of cardiovascular disease, and we identified Aminopyridine 2 as a potent tool.

Acknowledgments

We thank Samantha Plonsky, Eric Fortier, Jian Hong, Chenhui Zeng, Jay Larrow, and Keith Hoffmaster for contributions to the project; and Jason Elliot, Gerry Waters, and Jennifer Allport-Anderson for critical review of the manuscript.

Authorship Contributions

Participated in research design: Marro, Patterson, Lee, Deng, Reynolds, Ren, Axford, Patnaik, Hollis-Symynkywicz, Casson, Custeau, Ames, Loi, Zhang, Honda, Blank, Harrison, Papillon, Hamann, Marcinkeviciene, and Regard.

Conducted experiments: Patterson, Lee, Reynolds, Ren, Axford, Patnaik, Hollis-Symynkywicz, Casson, Custeau, Ames, Loi, Zhang, Honda, Harrison, and Regard.

Performed data analysis: Marro, Patterson, Lee, Deng, Ren, Axford, Patnaik, Hollis-Symynkywicz, Casson, Custeau, Ames, Loi, Zhang, Honda, Blank, Harrison, Papillon, and Regard.

Wrote or contributed to the writing of the manuscript: Marro, Patterson, Lee, Deng, Reynolds, Ren, Axford, Patnaik, Hollis-Symynkywicz, Ames, Zhang, Blank, Harrison, Papillon, Hamann, Marcinkeviciene, and Regard.

References

- Askari AT, Brennan ML, Zhou X, Drinko J, Morehead A, Thomas JD, Topol EJ, Hazen SL, and Penn MS (2003) Myeloperoxidase and plasminogen activator inhibitor 1 play a central role in ventricular remodeling after myocardial infarction. *J Exp Med* **197**:615–624.
- Brennan ML, Anderson MM, Shih DM, Qu XD, Wang X, Mehta AC, Lim LL, Shi W, Hazen SL, Jacob JS, et al. (2001) Increased atherosclerosis in myeloperoxidase-deficient mice. *J Clin Invest* **107**:419–430.
- Castellani LW, Chang JJ, Wang X, Lusic AJ, and Reynolds WF (2006) Transgenic mice express human MPO -463G/A alleles at atherosclerotic lesions, developing hyperlipidemia and obesity in -463G males. *J Lipid Res* **47**:1366–1377.
- Chung A, Marshall CV, Sin DD, Bolton S, Zhou S, Thain K, Cadogan EB, Maltby J, Soars MG, Mallinder PR, et al. (2012) Late intervention with a myeloperoxidase inhibitor stops progression of experimental chronic obstructive pulmonary disease. *Am J Respir Crit Care Med* **185**:34–43.
- Copeland RA (2005) Evaluation of enzyme inhibitors in drug discovery. A guide for medicinal chemists and pharmacologists. *Methods Biochem Anal* **46**:1–265.
- Dong JQ, Varma MV, Wolford A, Ryder T, Di L, Feng B, Terra SG, Sagawa K, and Kalgutkar AS (2016) Pharmacokinetics and disposition of the thiouracil derivative PF-06282999, an orally bioavailable, irreversible inactivator of myeloperoxidase enzyme, across animals and humans. *Drug Metab Dispos* **44**: 209–219.
- Ehrenfeld P, Matus CE, Pavicic F, Toledo C, Nualart F, Gonzalez CB, Burgos RA, Bhoola KD, and Figueroa CD (2009) Kinin B1 receptor activation turns on exocytosis of matrix metalloproteinase-9 and myeloperoxidase in human neutrophils: involvement of mitogen-activated protein kinase family. *J Leukoc Biol* **86**: 1179–1189.
- Eiserich JP, Baldus S, Brennan ML, Ma W, Zhang C, Tousson A, Castro L, Lusic AJ, Nauseef WM, White CR, et al. (2002) Myeloperoxidase, a leukocyte-derived vascular NO oxidase. *Science* **296**:2391–2394.
- Franck T, Kohlen S, Boudjeltia KZ, Van Antwerpen P, Bosseloir A, Niesten A, Gach O, Nys M, Deby-Dupont G, and Serteyn D (2009) A new easy method for specific measurement of active myeloperoxidase in human biological fluids and tissue extracts. *Talanta* **80**:723–729.
- Geoghegan KF, Varghese AH, Feng X, Bessire AJ, Conboy JJ, Ruggeri RB, Ahn K, Spath SN, Filippov SV, Conrad SJ, et al. (2012) Deconstruction of activity-dependent covalent modification of heme in human neutrophil myeloperoxidase by multistage mass spectrometry (MS⁴). *Biochemistry* **51**: 2065–2077.
- Haslacher H, Perkmann T, Gruenewald J, Exner M, Eandler G, Scheichenberger V, Wagner O, and Schillinger M (2012) Plasma myeloperoxidase level and peripheral arterial disease. *Eur J Clin Invest* **42**:463–469.

- Johnström P, Bergman L, Varnäs K, Malmquist J, Halldin C, and Farde L (2015) Development of rapid multistep carbon-11 radiosynthesis of the myeloperoxidase inhibitor AZD3241 to assess brain exposure by PET microdosing. *Nucl Med Biol* **42**:555–560.
- Jucaite A, Svenningsson P, Rinne JO, Cselényi Z, Varnäs K, Johnström P, Amini N, Kirjavainen A, Helin S, Minkwitz M, et al. (2015) Effect of the myeloperoxidase inhibitor AZD3241 on microglia: a PET study in Parkinson's disease. *Brain* **138**:2687–2700.
- Kaindlstorfer C, Sommer P, Georgievska B, Mather RJ, Kugler AR, Poewe W, Wenning GK, and Stefanova N (2015) Failure of neuroprotection despite microglial suppression by delayed-start myeloperoxidase inhibition in a model of advanced multiple system atrophy: clinical implications. *Neurotox Res* **28**:185–194.
- Klebanoff SJ (2005) Myeloperoxidase: friend and foe. *J Leukoc Biol* **77**:598–625.
- Kutter D, Devaquet P, Vanderstocken G, Paulus JM, Marchal V, and Gothot A (2000) Consequences of total and subtotal myeloperoxidase deficiency: risk or benefit? *Acta Haematol* **104**:10–15.
- Marsche G, Zimmermann R, Horiuchi S, Tandon NN, Sattler W, and Malle E (2003) Class B scavenger receptors CD36 and SR-BI are receptors for hypochlorite-modified low density lipoprotein. *J Biol Chem* **278**:47562–47570.
- McMillen TS, Heinecke JW, and LeBoeuf RC (2005) Expression of human myeloperoxidase by macrophages promotes atherosclerosis in mice. *Circulation* **111**:2798–2804.
- Nussbaum C, Klinke A, Adam M, Baldus S, and Sperandio M (2013) Myeloperoxidase: a leukocyte-derived protagonist of inflammation and cardiovascular disease. *Antioxid Redox Signal* **18**:692–713.
- Rudolph TK, Wipper S, Reiter B, Rudolph V, Coym A, Detter C, Lau D, Klinke A, Friedrichs K, Rau T, et al. (2012) Myeloperoxidase deficiency preserves vasomotor function in humans. *Eur Heart J* **33**:1625–1634.
- Ruggeri RB, Buckbinder L, Bagley SW, Carpino PA, Conn EL, Dowling MS, Fernando DP, Jiao W, Kung DW, Orr ST, et al. (2015) Discovery of 2-(6-(5-Chloro-2-methoxyphenyl)-4-oxo-2-thioxo-3,4-dihydropyrimidin-1(2H)-yl)acetamide (PF-06282999): a highly selective mechanism-based myeloperoxidase inhibitor for the treatment of cardiovascular diseases. *J Med Chem* **58**:8513–8528.
- Schultz J and Kaminker K (1962) Myeloperoxidase of the leucocyte of normal human blood. I. Content and localization. *Arch Biochem Biophys* **96**:465–467.
- Shao B, Oda MN, Oram JF, and Heinecke JW (2010) Myeloperoxidase: an oxidative pathway for generating dysfunctional high-density lipoprotein. *Chem Res Toxicol* **23**:447–454.
- Stefanova N, Georgievska B, Eriksson H, Poewe W, and Wenning GK (2012) Myeloperoxidase inhibition ameliorates multiple system atrophy-like degeneration in a transgenic mouse model. *Neurotox Res* **21**:393–404.
- Sugiyama S, Kugiyama K, Aikawa M, Nakamura S, Ogawa H, and Libby P (2004) Hypochlorous acid, a macrophage product, induces endothelial apoptosis and tissue factor expression: involvement of myeloperoxidase-mediated oxidant in plaque erosion and thrombogenesis. *Arterioscler Thromb Vasc Biol* **24**:1309–1314.
- Tidén AK, Sjögren T, Svensson M, Bernlind A, Senthilmohan R, Auchère F, Norman H, Markgren PO, Gustavsson S, Schmidt S, et al. (2011) 2-thioxanthines are mechanism-based inactivators of myeloperoxidase that block oxidative stress during inflammation. *J Biol Chem* **286**:37578–37589.
- Wang Y, Rosen H, Madtes DK, Shao B, Martin TR, Heinecke JW, and Fu X (2007) Myeloperoxidase inactivates TIMP-1 by oxidizing its N-terminal cysteine residue: an oxidative mechanism for regulating proteolysis during inflammation. *J Biol Chem* **282**:31826–31834.
- Zhang C, Patel R, Eiserich JP, Zhou F, Kelpke S, Ma W, Parks DA, Darley-Usmar V, and White CR (2001) Endothelial dysfunction is induced by proinflammatory oxidant hypochlorous acid. *Am J Physiol Heart Circ Physiol* **281**:H1469–H1475.
- Zheng W, Warner R, Ruggeri R, Su C, Cortes C, Skoura A, Ward J, Ahn K, Kalgutkar A, Sun D, et al. (2015) PF-1355, a mechanism-based myeloperoxidase inhibitor, prevents immune complex vasculitis and anti-glomerular basement membrane glomerulonephritis. *J Pharmacol Exp Ther* **353**:288–298.

Address correspondence to: Dr. Jean B. Regard, Novartis Institutes for Biomedical Research, 22 Windsor St., 3D310, Cambridge, MA 02139. E-mail: jean.regard@novartis.com
